Iranian Journal of Medical Physics

ijmp.mums.ac.ir

Backpropagation Neural Network Implementation in Volumetric Modulated Arch Therapy of Brain Cancer Dose Prediction

Nafisa Imtiyaziffati Rasoma Muliarso[1], Prawito Prajitno[2], Dewa Ngurah Yudhi Prasada[2], Aloysius Mario Yudi Putranto[2], Muhammad Fadli[2], Dwi Seno K. Sihono[1*]

1. Department of Physics, Faculty of Mathematics and Natural Sciences, Universitas Indonesia, Depok, West Java, 16424, Indonesia
2. Department of Radiation Oncology, MRCCC Siloam Hospital Semanggi, Jakarta, 12930, Indonesia

ARTICLE INFO

Article type:
Original Paper

Article history:
Received: June 06, 2024
Accepted: Dec 18, 2024

Keywords:
Artificial Intelligence
Volumetric Modulated Arc Therapy
Neural Network
Radiomics

ABSTRACT

Introduction: The quality of volumetric modulated arc therapy (VMAT) planning is highly subjective and varies due to differences in planner's experience. This process is time-consuming and involves multiple iterations to achieve clinical goals. Recent advancements in artificial intelligence (AI) offers an objective approach to improve the efficiency of VMAT planning.

Material and Methods: In this study, the backpropagation neural network with 5-fold cross-validation model was employed to train the extracted Radiomics and dosiomics features from organ contours DICOM RT structure and dose distribution DICOM RT dose using 178 VMAT technique brain cancer patients. The Radiomics and dosiomics features represent the organ shapes and dose distribution quantitatively to increase the prediction accuracy. The Mean Squared Error and paired t-test was used in model evaluation. The treatment planning quality parameters, homogeneity index (HI) and conformity index (CI), was evaluated from both predicted and clinical dose.

Results: The paired t-test indicated no significant differences (p-value > 0.05) in organs at risk (OAR) and planning target volume (PTV). The p-value for the left optic nerve is the lowest among average dose (D_{mean}) and maximum dose (D_{max}), respectively 0.1456 and 0.0662. The average HI was 0.084±0.036 (predicted) and 0.089±0.073 (clinical), and CI was 0.938±0.107 (predicted) and 0.957±0.136 (clinical).

Conclusion: The p-value for predicted parameters suggest that neural network-based dose prediction using Radiomics and dosiomics features produces results comparable to the manual treatment planning by medical physicists (overall testing dataset MSE = 0.0355).

► *Please cite this article as:*
Muliarso NIR, Prajitno P, Prasada DNY, Putranto AMY, Fadli M, Sihono DSK. Backpropagation Neural Network Implementation in Volumetric Modulated Arch Therapy of Brain Cancer Dose Prediction. Iran J Med Phys 2025; 22: 89-97. 10.22038/ijmp.2025.80324.2410.

Introduction

Advanced techniques in radiotherapy, such as intensity modulated radiation therapy (IMRT) and volumetric modulated arc therapy (VMAT), offer more conformal dose distribution to minimize excessive radiation doses to surrounding healthy tissue [1-2]. This is achieved through the use of multi-leaf collimator (MLC) modulation and gantry rotation, particularly in the VMAT technique [3]. However, these advanced treatment techniques have several drawbacks in the planning process. The optimization process is time-consuming and relies on an iterative trial and error process to achieve clinical goals for planning target volume (PTV) and organ at risk (OAR). This is because the set of descriptors, such as dose constraints set by planners are based on previous studies and are not specific to individual cases. Consequently, the quality of treatment planning is subjectively dependent on the experience of planners [4].

In order to simplify and reduce the planning time also subjectivity of the planning process, several studies proposed the use of a knowledge-based planning (KBP) algorithm that has the ability to define the relationship between the dose received by OAR and PTV according to the geometric structure involved in radiation therapy planning. The model obtained was used to predict the best therapy planning parameter for new patients with similar characteristics, and then the plan evaluation was done using dose volume histogram (DVH) [5].

Machine learning (ML) is also employed for data training in KBP to predict outcomes such as dose received by organs based on the organ features with specific prioritized planning parameter during evaluation to determine the quality of treatment planning [6-7]. Several parameters need to be considered to quantitatively evaluate the performance of treatment planning, including DVH, calculation of the conformity index (CI) which indicates how well the dose coverage received by the target volume, and calculation of the homogeneity index (HI) to analyze the uniformity of dose distribution within target volume [8-9].

*Corresponding Author: Tel: +62-21-7872610; Email: dwi.seno@sci.ui.ac.id

Radiomics features can be utilized as an input for ML model and obtained by converting image data into high-dimensional spatial features so that the organ structures including the tumor lesion and healthy organ can be obtained quantitatively [10]. The Radiomics feature extraction process can be conduct by carrying out image acquisition and pre-processing, delineating tumors and organs, performing feature extraction and feature selection, and then constructing a model [11]. One of the results of radiation therapy planning is dose distribution which has no ability to provide accurate evaluation using visual assessment only, so a quantitative approach is needed to describe dose distribution based on the dose level received by a specific organ volume that is known as a dosiomics features. By combining radiological image and dosimetry characteristics, information regarding the quality of the therapy plan can be obtained more comprehensively and increase the accuracy of predictions [12].

Previous studies have demonstrated the implementation of machine learning for determining the treatment quality parameters in head and neck cancer, such as nasopharynx cancer, achieved results that are equally good with those manually planned treatment [13-15]. Additionally, several studies have explored the use of machine learning for dose prediction in gynecologic cancer, such as cervical cancer [16-17]. Comparisons between KBP using Rapid Plan software and machine learning approaches have also been investigated in head and neck as well as prostate cancers and showed on par ability of machine learning [18-19]. However, only few studies have explored the used of Radiomicss and dosiomicss features for dose distribution prediction using machine learning. Therefore, this study will analyze backpropagation neural network utility as a method to predict the dose distribution in VMAT brain cancer patients. The proposed backpropagation neural network algorithm addressed the variability and subjectivity of VMAT planning proses by automating dose prediction. By using Radiomics and dosiomics features as inputs, the model directly integrates patient-specific optimization parameters, reducing the need for repeated manual adjustments, and able to shortens the therapy planning process and minimizes the subjectivity influenced by the planner's experience. However, scalability of integrating AI into VMAT planning clinically requires proper computational resources and data standardization to ensure consistency in treatment delivery.

Materials and Methods

Patients data collection

Clinically administered VMAT radiation therapy treatment plans for 178 brain cancer patients at MRCCC Siloam Hospitals, Semanggi, spanning from 2011 to 2024, were analyzed. The dataset comprised Digital Imaging and Communication in Medicine (DICOM) CT with imaging of specific organs acquired from CT scans of patients, DICOM RT structure with contour images delineated by radiation oncologist, and DICOM RT dose file containing information on the clinically administered and received doses by organ volume and can be visualized into dose volume histogram (DVH) for the treatment planning quality evaluation process. All treatment plans were created using the Varian Eclipse v13.6 treatment planning system (TPS) with the beam energy used at 6 MV to decrease low dose scatter in the body and a dose rate of 600 MU to compensate for the dose rate modulation for smooth gantry rotation movement and not burdening the linear accelerator (linac) motor. The overview of the data used in this study is shown in Table 1.

Table 1. The treatment planning data used and available overview

Total data	Total fraction	Dose/fraction (cGy)	Total dose (cGy)
178	5-30	200	1000-6000

Twelve Radiomics shape features for specific OAR and the PTV were extracted from DICOM CT and DICOM structure files using 3D slicer software based on the PyRadiomicss library [20]. These features characterized the shape of organs based on delineation information. Dosiomics features from DICOM dose files were extracted by using the dose volume histogram module provided in 3D slicer software for the doses received by 2%, 98%, and 50% of the organ volumes ($D_{2\%}$, D_{98}%, and $D_{50\%}$). Additionally, the volumetric data consisting of the target volume and the total target volume that received 95% of the prescribed dose (V_{PTV} and $V_{95\%}$) were assessed. Maximum doses (D_{max}), minimum doses (D_{min}), and average doses (D_{mean}) for organs at risk were also extracted. The specific organs evaluated in this study included the left and right eyes, left and right optic nerves, left and right lenses, brainstem, and the cancer lesion (PTV) [21]. 3D slicer provides a comprehensive set of tools for segmentation, Radiomics feature extraction through PyRadiomicss library, and visualization. Additionally, 3D Slicer offers flexibility in handling a variety of medical imaging formats, particularly DICOM.

Missing values in the dataset were handled using mean imputation, where any missing entries in a feature are replaced with the mean value of that feature. This approach ensures that the dataset remains complete and retains consistent across all features, preventing potential biases or errors during model training. By filling missing values with a representative statistic, mean imputation enabling the model to learn effectively from the full dataset and ensuring reliable and accurate predictions of neural network algorithm. Normalization of the dosiomics features was performed relative to the dose prescription value, ensuring the data ranged between 0 and 1. Furthermore, the normalization for volumetric data was carried out relative to the PTV volume.

Neural-network architecture building

The dataset was split into 70% training-validation dataset and 30% testing dataset. During the training and validation process, 5-fold cross-validation was implemented to mitigate the limitations of the available data and prevent the model from overfitting, as shown in Figure 1.

The Radiomics dataset was normalized using equation (1) to scale each feature within the 0 and 1 range.

$$X' = \frac{X - X_{min}}{X_{max} - X_{min}} \quad (1)$$

Where X_{min} and X_{max} are the minimum and maximum values of the features in each column.

The feedforward propagation utilized random weight to determine the number of neurons in the input layer, hidden layer, and output layer. The activation function used was rectified linear unit (ReLU), chosen for its efficiency in capturing complex non-linear relationships while offering computational simplicity. ReLu activates neurons only when certain condition were met, such as the input is positive, a property that reduces the computational burden to a simple thresholding operation. This not only accelerates the model's learning process but also makes it highly effective in handling the intricacies of non-linear data patterns. The loss function described by the mean squared error between predicted doses and clinical doses can be calculated using equation (2).

$$MSE = \frac{1}{n}\sum_{i=1}^{n}(y_i - \hat{y}_i)^2 \quad (2)$$

Where n is the number of samples, y_i is the predicted dose, and $\hat{y}_i$ is the actual dose.

In the backpropagation process, the gradient of the loss with respect to the weights are then updated using the adaptive moment estimation (Adam) optimizer which adjusts the weights using equation (3). Adam optimizer algorithm modify the learning rate for each coordinate according to past gradient data, and autonomously select suitable learning rates to ensure rapid convergence during training with smaller number of tuning the hyper-parameters [22]. This procedure is carried out repeatedly over several epochs to reduce the loss and enhance the accuracy of the model. Adam was chosen as the optimizer for this study due to its ability to maintain a moving average of both the first moment and second moment, helping to avoid local minima and enhance performance. Additionally, Adam effectively handles sparse gradients in the relationship between Radiomics and dosiomics features, advantageous for dose prediction [23]. The process of hyper-parameter tuning followed a trial and error approach, balancing model complexity with computational efficiency to optimize VMAT dose prediction accuracy. Setting the number of epochs to 500 allowed the model ample time to learn and achieve convergence without overfitting. The choice of 100 hidden layer size provided the necessary complexity to capture intricate relationships between Radiomics and dosiomics features, ensuring the model can effectively represent non-linear patterns while maintaining computational manageability. This configuration enabled the model to generalize well while preventing excessive computational burden. The model then trained and validated across 5 folds, ensuring that each subset of the data is used for validation exactly once [24]. This helps in assessing the performance of model, where the total of 54 patients were used as an unseen testing dataset, to assess the model performance.

$$\theta_{t+1} = \theta_t - \eta \cdot \frac{\hat{w}_t}{\sqrt{\hat{v}_t} + \varepsilon} \quad (3)$$

Where θ_t represents the weights at step t, η is the learning rate, $\hat{w}_t$ is the bias-corrected first moment estimate, $\hat{v}_t$ is the bias-corrected second moment estimate, and ε is a small constant to prevent division by zero. The training and validation loss curve was used to evaluate the backpropagation neural network model over epoch for fold 1, shown in Figure 2.

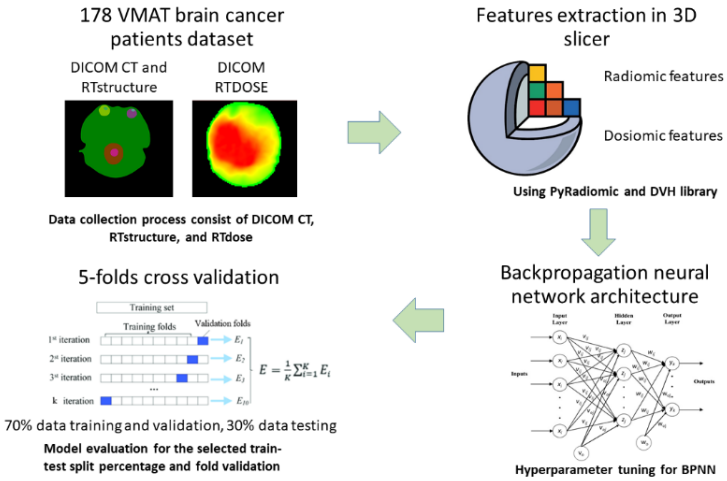

Figure 1. Workflow from data collection to backpropagation neural network architecture building

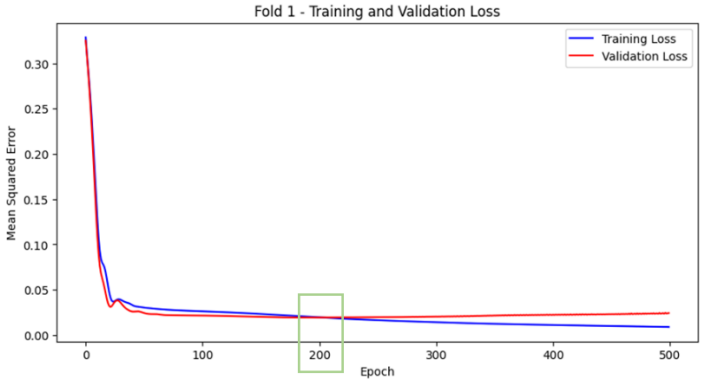

Figure 2. Training and validation loss curve for fold 1

Model evaluation

Predicted maximum doses (D_{max}) and average doses (D_{mean}) for OAR were compared with clinical doses data as a ground truth. The quality of planning for PTV was evaluated using the CI and the HI. According to the International Commission on Radiation Unit (ICRU) report No. 83, a CI value defined as equation (4) that is close to 1 indicates better coverage in target volume and a HI value defined as equation (5) that is close to 0 indicates the better dose homogeneity for target volume (9).

$$CI = \frac{V_{95\%}}{V_{PTV}} \quad (4)$$

$$HI = \frac{D_{2\%} - D_{98\%}}{D_{50\%}} \quad (5)$$

Where,

$V_{95\%}$: volume PTV received 95% prescribed dose

V_{PTV}: total volume of PTV

$D_{x\%}$: dose received by x% volume PTV

The significance of the difference between predicted and clinical doses was assessed using a paired t-test to compare the means of two datasets. A *p*-value greater than 0.05 indicates that the mean difference between the two datasets is considered to be not statistically significant different to 0.

Results

Predicted dose of Organs at risk (OAR)

The maximum dose (D_{max}), average dose (D_{mean}), and minimum dose (D_{min}) received by each organ at risk (OAR) observed was displayed in Table 2, Table 3 and Table 4. The study findings indicate that there is no substantial difference between the clinical dose and the predicted dose, as the *p*-value exceed 0.05.

Table 2. Comparison of maximum dose (D_{max}) for clinical and predicted.

Organ structure	Parameter (mean±SD)		Mean Squared Error (MSE)	p-value
	D_{max}			
	Clinical	Predicted		
Left eye	0.376±0.212	0.387±0.190	0.0456	0.4219
Right eye	0.384±0.217	0.393±0.243	0.0702	0.7952
Left optic nerve	0.526±0.266	0.565±0.302	0.0839	0.0662*
Right optic nerve	0.561±0.298	0.619±0.319	0.1281	0.2221
Right lens	0.105±0.060	0.112±0.053	0.0053	0.5126
Left lens	0.105±0.058	0.112±0.046	0.0050	0.4059
Brainstem	0.856±0.189	0.892±0.099	0.0377	0.1766

* Lowest *p*-value

Table 3. Comparison of average dose (D_{mean}) for clinical and predicted.

Organ structure	Parameter (mean±SD)		Mean Squared error (MSE)	p-value
	D_{mean}			
	Clinical	Predicted		
Left eye	0.150±0.091	0.161±0.082	0.0093	0.4219
Right eye	0.154±0.094	0.162±0.106	0.0163	0.6549
Left optic nerve	0.382±0.232	0.431±0.252	0.0612	0.1456*
Right optic nerve	0.406±0.251	0.430±0.288	0.0963	0.5767
Right lens	0.088±0.050	0.089±0.047	0.0032	0.7968
Left lens	0.088±0.049	0.088±0.040	0.0024	0.9542
Brainstem	0.588±0.261	0.611±0.272	0.0772	0.5450

Table 4. Comparison of minimum dose (D_{min}) for clinical and predicted.

Organ structure	Parameter (mean±SD) D_{min}		MSE	p-value
	Clinical	Predicted		
Left eye	0.065±0.039	0.061±0.033	0.0018	0.5578
Right eye	0.065±0.038	0.060±0.041	0.0019	0.4428*
Left optic nerve	0.226±0.150	0.241±0.157	0.0335	0.5499
Right optic nerve	0.239±0.163	0.237±0.178	0.0477	0.9591
Right lens	0.076±0.044	0.076±0.043	0.0030	0.9256
Left lens	0.077±0.043	0.080±0.040	0.0026	0.6725
Brainstem	0.333±0.314	0.312±0.325	0.1060	0.6342

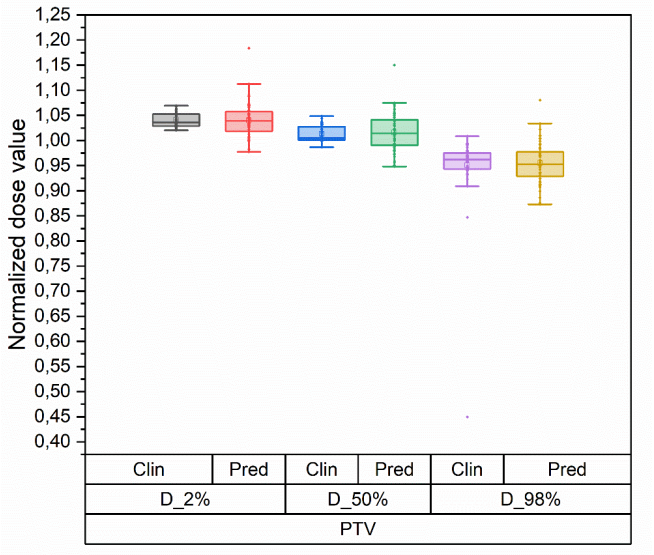

Figure 3. Comparison between clinical and predicted dosiomics features for planning target volume (PTV)

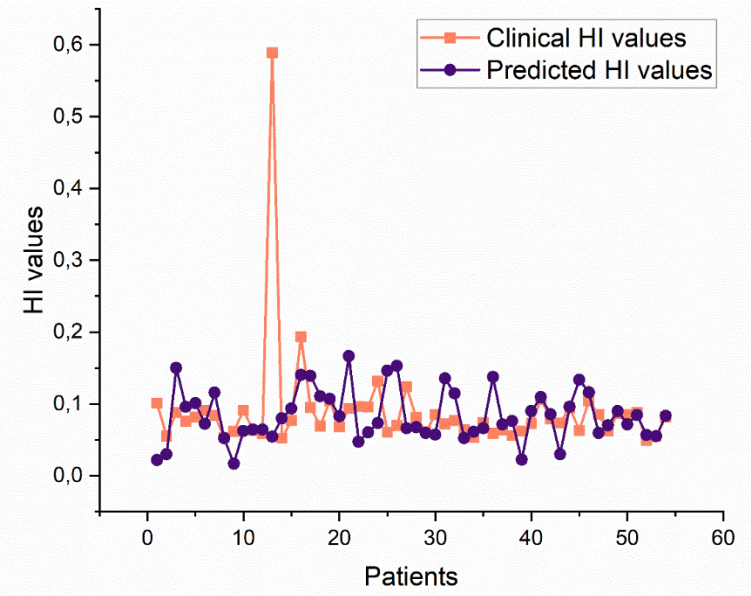

Figure 4. Homogeneity index (HI) value comparison between clinical and predicted dosiomics features

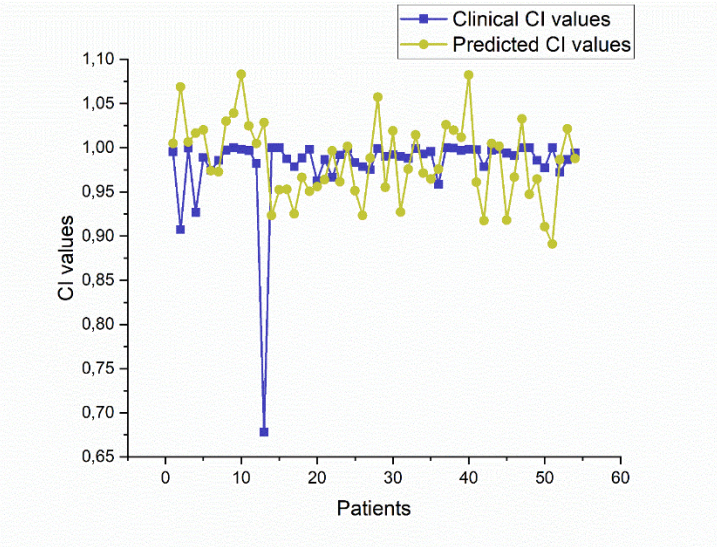

Figure 5. Conformity index (CI) value comparison between clinical and predicted dosiomics features

Predicted dose of Planning Target Volume (PTV)

The statistical data distribution for both clinical and predicted dosiomics features of PTV was shown in Figure 3. Based on the gathered data, there was no significant difference between the median values of clinical and predicted dosiomics features of PTV, as confirmed by the mean squared error (MSE) and the *p*-value detailed in Table 5.

Treatment planning quality parameters

Treatment planning quality parameter, homogeneity index (HI) and conformity index (CI), for clinical and predicted value in PTV was determined using equation (4) and (5). Subsequently, the outcomes were compared, as illustrated in Figure 4 and Figure 5.

Discussion

The 178 treatment planning data for brain cancer radiation therapy using volumetric modulated arc therapy (VMAT) consist of DICOM CT containing organ-specific image acquisition with a CT simulator at the beginning of the therapy planning process. It also encompasses DICOM structure containing delineation information performed by the radiation oncologist to differentiate between organ structures, and also DICOM dose which detailing the dose distribution received by the organ. From the overall DICOM file, by using pyRadiomics and dose volume histogram modules in 3D Slicer software, the Radiomics and dosiomics features can be extracted. The pre-processing is done to prepare the data for the training and validation process. The dosiomics features need to undergo normalization relative to dose prescription before carrying out the training process.

For organs at risk (OAR), the maximum dose (D_{max}) and average dose (D_{mean}) were evaluated during the treatment planning process to avoid excessive radiation dose exposure that could impair organ function. The minimum dose (D_{min}) was used for recording and reporting purposes in compliance with ICRU report No. 83 requirements.

The combination of Radiomics and dosiomics features offers comprehensive insights into the dose distribution within specific organ volumes. These features enable the model to account for each patient's unique anatomy and dosimetric requirements, enabling the prediction of dose to be customized to the individual clinical situation.

The training and validation loss curve was used to evaluate the backpropagation neural network model over epoch for fold 1, as shown in Figure 2, where the loss curve interseceted around epoch 200. This intersection indicated that the model had reached a point where it performed similarly on both training and validation data, suggesting well generalization. After this point, the validation loss showed a slight upward trend while the training loss continues to decrease. This pattern suggests that the model was further refining its understanding of the training data while maintaining a balance with generalization of unseen data in training dataset.

The backpropagation neural network model achieved a comparable predicted dose with hand-crafted clinical dose, as shown in Table 2, Table 3, and Table 4, no *p*-value was lower than 0.05, indicating there was no significant difference between the predicted dosiomics features with the clinical dose. The *p*-value for the left optic nerve is the lowest among the average dose (D_{mean}) and maximum dose (D_{max}). However, it remains above the typical significance level of 0.05, suggesting that, although the difference is relatively notable, it is not statistically significant, due to several factors, such as in clinical setting, many of the left optic nerve structure organs were overlapping with the PTV, resulting the data used for ML architecture not following a normal distribution. The Radiomics data used as input, particularly for the spherical feature of the left optic nerve, holds the smallest value among other organs at risk (OAR), 0.62166.

Table 5. Comparison of dosiomics features in PTV homogeneity

Dosiomics features	Parameter (mean±SD)		MSE	p-value
	Clinical	Predicted		
$D_{2\%}$	1.041±0.015	1.039±0.034	0.0009	0.8288
$D_{50\%}$	1.013±0.014	1.016±0.038	0.0012	0.5356*
$D_{98\%}$	0.950±0.074	0.955±0.041	0.0066	0.6895

The spherical features value for the right optic nerve, right eye, left eye, right lens, left lens, and brainstem are, respectively, 0.623247; 0.87266; 0.873851; 0.815868; 0.812168; and 0.715863. The spherical Radiomics shape features reflects how closely an organ's structure resembles a sphere, with values closer to zero indicating increased deviation from a spherical shape, implying greater complexity of the organ's structure. For D_{min} parameter, the lowest *p*-value was right eye. D_{min} parameter represents the dose minimum received by volume organ. The slight difference of *p*-value for D_{min} parameter was due to the variability of the D_{min} received by volume organ. In the treatment planning process, medical physicists set the optimization descriptor that includes dose constrain for OAR and PTV. The spatial relationship and proximity between the sensitive OAR and PTV will affect the ability of the treatment planning system (TPS) algorithm to achieve clinical goals, which aim to deliver the highest dose possible to PTV while sparing the dose received by OAR [25].

The dosiomics featured observe for PTV consists of the dose received by 2% volumes ($D_{2\%}$), the dose received by 50% volumes ($D_{50\%}$), and the dose received by 98% volumes ($D_{98\%}$). Analysis of the PTV dosiomics features, depicted in Figure 3, suggested that the median between clinical and predicted doses are closely aligned. The lower and upper quartiles that are indicated by the upper and lower border of the box represent the coordinates which half of the data lies. An outlier for clinical data as noted in the testing data, stemming from the use of the only sub-optimal VMAT brain cancer treatment planning data available in the database of the hospital, where the 95% dose prescription only covered around 89% PTV where the supposed coverage is 98% PTV, to verify the capability of the model in providing an objective overview for dose distribution. These findings for the *p*-value from the paired t-test and MSE parameters, demonstrate that the difference between clinical and predicted doses is not significant, as shown in Table 5 and it also show that the sub-optimal Radiomics information (patient 13 in Figure 4 and 5) can effectively predict the optimal dosiomics features of testing data with favorable results and improved dose uniformity and coverage in PTV that is represented by the treatment planning quality parameters, HI and CI, as shown in Figure 4 and Figure 5. The noted outliers in predicted dosiomics features of PTV were due to the large anatomical variance for PTV Radiomics features with different locations and tumor sizes [26]. The average for predicted HI value is 0.084±0.036 and 0.089±0.073 for the clinical HI value (*p*-value = 0.6222). The average predicted CI value achieved is 0.938±0.107 compared to 0.957±0.136 for clinical CI value (*p*-value = 0.4164), where according to ICRU report No. 83, a HI values leaned towards 0 has better uniformity of dose distribution within the PTV and a CI values closer to 1 indicates better dose coverage for the PTV. The acceptable dose coverage in radiation therapy treatment planning process ranges from 95% and 107% with 98% of the PTV required to be covered by a minimum 95% of the prescribed dose. A high uniformity in dose distribution enhance effective dose tumour control to minimize the risk of recurrence by ensuring the entire PTV receives an adequate radiation dose [27]. The MSE value between the clinical and predicted dosiomics features in overall testing dataset was 0.0355, where small MSE implies better performance in backpropagation neural network model.

The observed discrepancy between the clinical and predicted dose distributions, which reflects lower model performance, may stem from the close spatial relationship between the PTV and OARs. The limitations of the available dataset's size and diversity, as a small dataset might not capture the full spectrum of clinical scenarios, will also decrease model performance to predict dose distribution. Additionally, potential biases may arise from the limitation of demographic variability, as this study was conducted at a single hospital. To further improve generalizability, future studies will incorporate larger, multicenter datasets to overcome possible biases that occur.

Conclusion

In this study, we utilized a backpropagation neural network model to predict the dose received by OAR and PTV based on the delineation information from DICOM RT structure and dose distribution data from DICOM RT dose. The results demonstrate the predicted dose obtained are comparable with hand-crafted clinical dose where the Mean Squared Error (MSE) for overall testing dataset was 0.0355. This show the potential used of backpropagation neural network model for dose prediction in radiotherapy. For further study, in order to improve model performance, the overlap or proximity between PTV and OARs need to be considered by incorporating 3D spatial and geometric information that indicates the proximity between the PTV and OARs. Additionally, increasing the size of training dataset can provide the model with more diverse examples, allowing it to better generalize and handle a wider variety of cases during the training process.

Acknowledgment

The authors sincerely appreciate the Department of Physics, Universitas Indonesia and the Department of Radiotherapy MRCCC Siloam Hospitals Semanggi, Jakarta for the support of this study.

References

1. Podgorsak EB. Radiation Physics for Medical Physicists [Internet]. Berlin, Heidelberg: Springer Berlin Heidelberg; 2010 [cited 2021 Mar 20].
2. Morris S, Roques T, Ahmad S, Loo S. Practical Radiotherapy Planning. Fifth Edit. CRC Press; 2024.
3. Shirato H, Le QT, Kobashi K, Prayongrat A, Takao S, Shimizu S, Giaccia A, Xing L, Umegaki K. Selection of external beam radiotherapy approaches for precise and accurate cancer treatment. Journal of Radiation Research. 2018 Mar 1;59(suppl_1):i2-10.
4. Zarepisheh M, Hong L, Zhou Y, Huang Q, Yang J, Jhanwar G, et al. Automated and Clinically Optimal Treatment Planning for Cancer Radiotherapy. INFORMS J Appl Anal. 2022;52(1):69–89.
5. Ge Y, Wu QJ. Knowledge-based planning for intensity-modulated radiation therapy: a review of data-driven approaches. Medical physics. 2019 Jun;46(6):2760-75.
6. Tseng HH, Luo Y, Ten Haken RK, El Naqa I. The Role of Machine Learning in Knowledge-Based Response-Adapted Radiotherapy. Front Oncol. 2018 Jul 27;8:367315.
7. Jensen PJ, Zhang J, Koontz BF, Wu QJ. A novel machine learning model for dose prediction in prostate volumetric modulated arc therapy using output initialization and optimization priorities. Frontiers in artificial intelligence. 2021 Apr 23;4:624038.
8. Vandewinckele L, Claessens M, Dinkla A, Brouwer C, Crijns W, Verellen D, van Elmpt W. Overview of artificial intelligence-based applications in radiotherapy: Recommendations for implementation and quality assurance. Radiotherapy and Oncology. 2020 Dec 1;153:55-66.
9. Menzel HG. The international commission on radiation units and measurements. Journal of the ICRU. 2012 Dec;12(2):1-2.
10. Van Griethuysen JJ, Fedorov A, Parmar C, Hosny A, Aucoin N, Narayan V, et al. Computational radiomics system to decode the radiographic phenotype. Cancer research. 2017 Nov 1;77(21):e104-7.
11. Kraus KM, Oreshko M, Schnabel JA, Bernhardt D, Combs SE, Peeken JC. Dosiomics and radiomics-based prediction of pneumonitis after radiotherapy and immune checkpoint inhibition: the relevance of fractionation. Lung Cancer. 2024 Mar 1;189:107507.
12. Qin Y, Zhu LH, Zhao W, Wang JJ, Wang H. Review of Radiomicss- and Dosiomicss-based Predicting Models for Rectal Cancer. Front Oncol. 2022;12(August):1–12.
13. Hu J, Liu B, Xie W, Zhu J, Yu X, Gu H, et al. Quantitative comparison of knowledge-based and manual intensity modulated radiation therapy planning for nasopharyngeal carcinoma. Frontiers in oncology. 2021 Jan 7;10:551763.
14. Sinha S, Kumar A, Maheshwari G, Mohanty S, Joshi K, Shinde P, et al. Development and Validation of Single-Optimization Knowledge-Based Volumetric Modulated Arc Therapy Model Plan in Nasopharyngeal Carcinomas. Advances in radiation oncology. 2024 Jan 1;9(1):101311.
15. Wang Y, Piao Z, Gu H, Chen M, Zhang D, Zhu J. Deep learning-based prediction of radiation therapy dose distributions in nasopharyngeal carcinomas: a preliminary study incorporating multiple features including images, structures, and dosimetry. Technology in Cancer Research & Treatment. 2024 May;23:15330338241256594.
16. Gronberg MP, Jhingran A, Netherton TJ, Gay SS, Cardenas CE, Chung C, et al. Deep learning–based dose prediction to improve the plan quality of volumetric modulated arc therapy for gynecologic cancers. Medical physics. 2023 Nov;50(11):6639-48.
17. Liu J, Zhang X, Cheng X, Sun L. A deep learning-based dose prediction method for evaluation of radiotherapy treatment planning. Journal of Radiation Research and Applied Sciences. 2024 Mar 1;17(1):100757.
18. Gronberg MP, Beadle BM, Garden AS, Skinner H, Gay S, Netherton T, et al. Deep learning–based dose prediction for automated, individualized quality assurance of head and neck radiation therapy plans. Practical radiation oncology. 2023 May 1;13(3):e282-91.
19. Kajikawa T, Kadoya N, Ito K, Takayama Y, Chiba T, Tomori S, et al. A convolutional neural network approach for IMRT dose distribution prediction in prostate cancer patients. Journal of radiation research. 2019 Sep;60(5):685-93.
20. Li S, Deng YQ, Zhu ZL, Hua HL, Tao ZZ. A comprehensive review on radiomics and deep learning for nasopharyngeal carcinoma imaging. Diagnostics. 2021 Aug 24;11(9):1523.
21. Puttanawarut C, Sirirutbunkajorn N, Tawong N, Jiarpinitnun C, Khachonkham S, Pattaranutaporn P, Wongsawat Y. Radiomic and dosiomic features for the prediction of radiation pneumonitis across esophageal cancer and lung cancer. Frontiers in Oncology. 2022 Feb 16;12:768152.
22. Liu M, Yao D, Liu Z, Guo J, Chen J. An improved Adam optimization algorithm combining adaptive coefficients and composite gradients based on randomized block coordinate descent. Computational intelligence and neuroscience. 2023;2023(1):4765891.
23. Mortazi A, Cicek V, Keles E, Bagci U. Selecting the best optimizers for deep learning–based medical image segmentation. Frontiers in Radiology. 2023 Sep 21;3:1175473.
24. Berrar D. Cross-validation. Encycl Bioinforma Comput Biol ABC Bioinforma. 2018 Jan 1;1–3:542–5.
25. Mao YP, Yin WJ, Guo R, Zhang GS, Fang JL, Chi F, et al. Dosimetric benefit to organs at risk following margin reductions in nasopharyngeal carcinoma treated with intensity-modulated radiation therapy. Cancer Communications. 2015 Dec;34(3):1-9.

26. Foster I, Spezi E, Wheeler P. Evaluating the use of machine learning to predict expert-driven pareto-navigated calibrations for personalised automated radiotherapy planning. Applied Sciences. 2023 Apr 3;13(7):4548.
27. Azharuddin SK, Kumar P, Navitha S, Chauhan AK, Kumar P, Nigam J, et al. Comparison of Dosimetric Parameters and Clinical Outcomes in Inversely Planned Intensity-Modulated Radiotherapy (IMRT) and Field-in-Field Forward Planned IMRT for the Treatment of Breast Cancer. Cureus. 2022 Jul 9;14(7).